Ito and Goshima, http://www.jcb.org/cgi/content/full/jcb.201507001/DC1

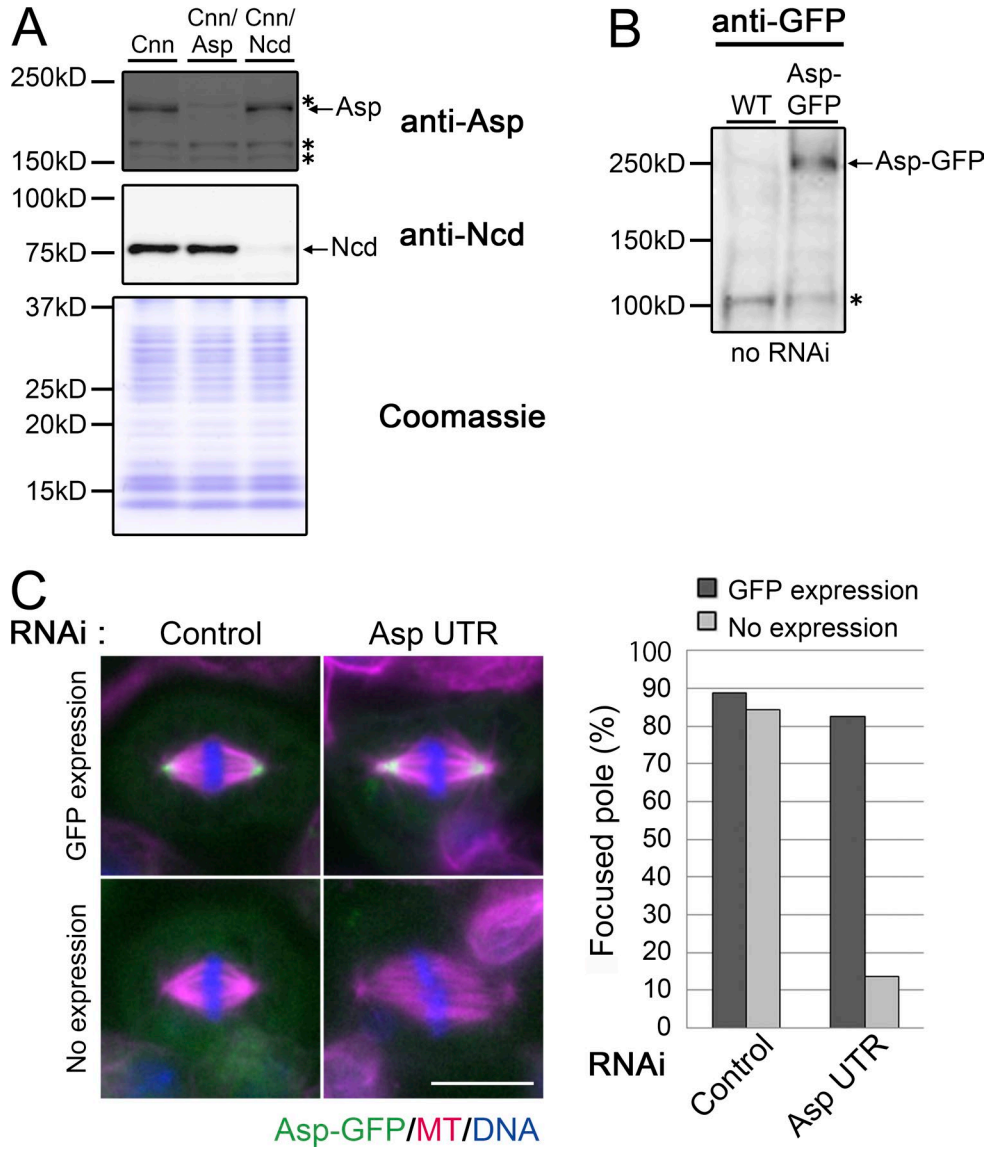

Figure S1. **RNAi knockdown confirmation and the functionality of the Asp-GFP fusion gene.** (A) Immunoblotting confirmed efficient knockdown of Ncd and Asp after RNAi. Cell extracts were prepared from the cell line expressing GFP-tubulin, which was used in Fig. 1 A. Quantification of band intensities indicated that >95% or 90% of endogenous Ncd or Asp was depleted, respectively. The asterisks indicate cross-reactions of anti-Asp antibody with unknown proteins. Coomassie staining served as the loading control. (B) Establishment of a cell line expressing Asp-GFP was confirmed by immunoblotting using the anti-GFP antibody (JL-8; Takara Bio Inc.). The asterisk indicates the cross-reaction of the antibody to an unknown protein. (C) Asp-GFP expression rescued the pole-unfocusing phenotype caused by endogenous Asp depletion using RNAi targeting the UTR (n = 23). The cell in this panel is identical to that presented in Fig. 3 A. Bar, 10 µm.

Table S1. **Primers for RNAi**

Gene	Primer sequences (5′ to 3′)
Control (pBluescript)	TAAATTGTAAGCGTTAATATTTTG
	AATTCGATATCAAGCTTATCGAT
Asp (exon)	CTTATTTACAAATTCCGCTCGC
	ACTTTCTCATTGAAAGCTTCGC
Asp (5′ UTR)[a]	CGACGCTCTAATTTGTTTAATTTTTGTTCG
	GGCGCTCATTGCAGGGAATGG
Asp (3′ UTR)[a]	ACATGTTTTAGATTTAGGAAAATTC
	TTTGACTTTCAATTGTCTTTATTCTTC

T7 promoter sequences (5′-TAATACGACTCACTATAGGG-3′) were attached to each end of the dsRNA sequences.
[a]5′ UTR and 3′ UTR sequences were fused and used as the UTR RNAi construct.

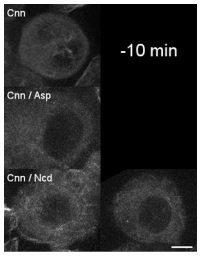

Video 1. **The distinct spindle MT–unfocusing phenotype after Asp or Ncd depletion.** GFP-tubulin was imaged in 3D every 1 min using spinning-disk confocal microscopy with RNAi-treated cells. Image sequences after maximum projection are presented. Spindle poles were never focused in the absence of Asp, whereas focusing was observed transiently after NEBD in the absence of Ncd. Time 0 corresponds to the time of NEBD. Bar, 5 µm.

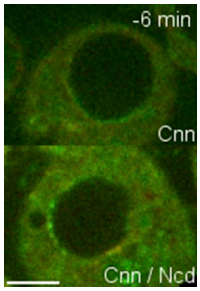

Video 2. **Asp-GFP is localized to the focusing point in the absence of Ncd.** Asp-GFP and mCherry-tubulin were imaged every 2 min with spinning-disk confocal microscopy in RNAi-treated cells. Time 0 corresponds to the time of NEBD. Bar, 5 µm.

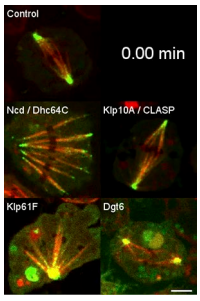

Video 3. **Poleward movement of Asp-GFP in the mitotic spindle.** Asp-GFP and mCherry-tubulin were imaged every 4.8 s with spinning-disk confocal microscopy in RNAi-treated cells. Note that intraspindle signals were rarely observed in the absence of Dgt6, an augmin subunit. Bar, 5 µm.

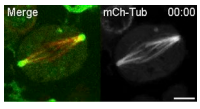

Video 4. **Poleward movement of Asp-GFP in the mitotic spindle depleted of centrosomes.** Asp-GFP and mCherry-tubulin were imaged every 5 s with spinning-disk confocal microscopy in Cnn RNAi–treated cells. Time is displayed in minutes/seconds. Bar, 5 µm.

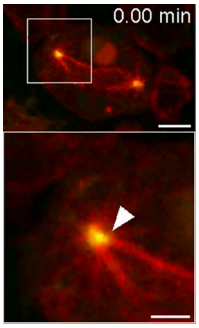

Video 5. **Polar enrichment of Asp-GFP in the absence of intraspindle MTs.** Asp-GFP and mCherry-tubulin were imaged every 4.8 s with spinning-disk confocal microscopy in Dgt6 (augmin) RNAi–treated cells. Punctate GFP signals were occasionally observed at the interior region of the centrosome (arrowhead in the magnified view [bottom]). Note that the cell in this video is identical to that presented in Video 3; less contrasted GFP signals are displayed in this video. Bars: (top) 5 μm; (bottom) 2 μm.

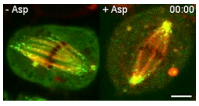

Video 6. **Unclustered MT minus ends at the pole in the absence of functional Asp.** AspΔC-GFP (left) or Asp(FL)-GFP (right) and mCherry-tubulin were imaged every 4 s with spinning-disk confocal microscopy in cells depleted of endogenous Asp. Time is displayed in minutes/seconds. Bar, 5 μm.

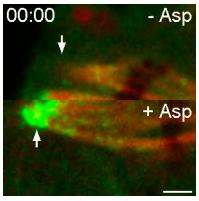

Video 7. **Asp-dependent focusing of intraspindle MTs.** AspΔC-GFP (top) or Asp(FL)-GFP (bottom) and mCherry-tubulin were imaged every 4 s with spinning-disk confocal microscopy in Asp RNAi–treated cells. Arrowheads indicate the minus ends of the outermost MT bundle, whereas arrows indicate the pole. Time is displayed in minutes/seconds. Bar, 2 μm.